Evaluation of the influence of the number of GCPS on the measurement quality of a photogrammetric block captured with an RTK UAV in geographical environments with high topographic roughness

di Kevin De Flué Pilco Lopez, Moisés Araca Chile

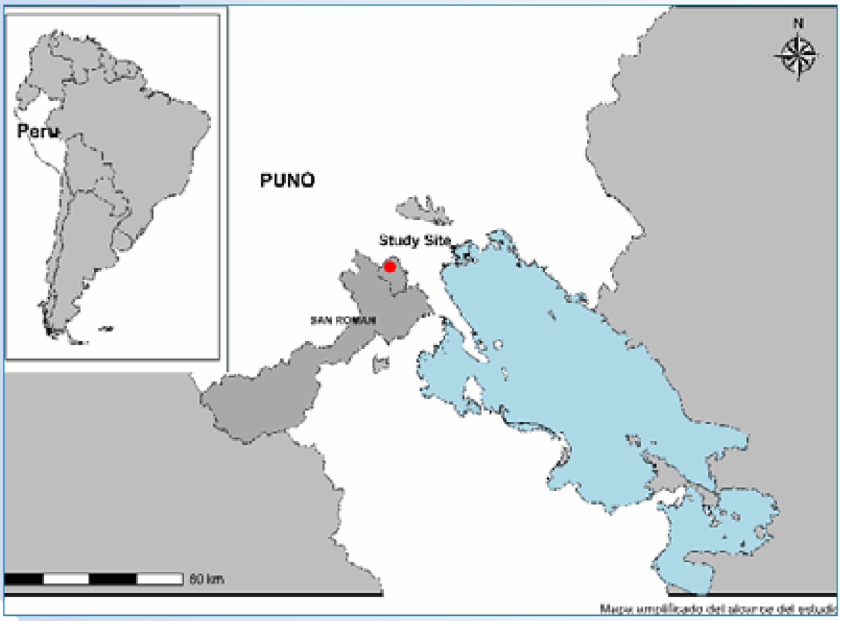

Fig. 1 - Study Area. Projection coordinate system: WGS_1984_UTM_zone_19S.

In recent times, digital photogrammetry has seen significant advancements in its application to topography. These advances are mainly due to the development of UAVs equipped with high-resolution cameras and more advanced sensors that capture images in different spectral bands, allowing for more detailed and precise terrain information. Additionally, the use of automatic matching algorithms and advanced processing software has streamlined the process of extracting topographic information from images (Benassi et al., 2017).

Despite technological and software advancements, it is crucial to consider various aspects to obtain precise and reliable results, such as the georeferencing method, the number of Ground Control Points (GCPs), the quality and resolution of images, the position and orientation of the camera, atmospheric conditions, the presence of shadows, and obstacles, among others (Elkhrachy, 2021). In UAV-captured imagery, two main georeferencing approaches are employed: direct and indirect (Padró et al., 2019). The indirect georeferencing method involves using GCPs to establish a relationship between their coordinates and the captured images. From this relationship, image georeferencing can be calculated to generate photogrammetric models (Elkhrachy, 2021). When applying this georeferencing method in complex geographical environments, logistical problems arise, ranging from inspection and access for GCP placement. These logistical aspects may require additional time and resources, affecting planning and execution (Stott et al., 2020a). Completely dispensing with GCPs can reduce time and, consequently, the costs of projects related to topographic surveying in complex geographical environments. Formally, direct georeferencing involves positioning the camera using onboard GNSS receivers enabled for RTK positioning, capable of producing photogrammetric models with centimeter-level accuracy, even if GCPs are not placed or measured, or if a local base receiver is not used. This provides an efficient and convenient solution in situations where time and accessibility are limited (Taddia et al., 2020) . RTK technology allows for more accurate determination of the camera's position and orientation during aerial image acquisition, offering a promising solution to reduce proportional dependence on

GCPs (Pourreza et al., 2022). The extensive body of literature using UAVs capable of direct georeferencing confirms the aforementioned. In the study conducted by (Stott et al., 2020b), it is affirmed that RTK-enabled UAVs can be used without any GCP to produce acceptable results, with a Root Mean Square Error (RMSE) in the Z-axis of about 0.07m. This was achieved with images captured using the cross-flight lines method to obtain adequate overlapping coverage in longitudinally extensive corridors. On the other hand, (Liu et al., 2022) obtained an RMSE in the Z-axis of 0.087m when no GCPs were used, achieved through direct georeferencing. Furthermore, the study by (Benassi et al., 2017), reports an RMSE in height of 0.095m using DG, confirming that this technique offers acceptable accuracy compared to other traditional georeferencing methods. It is important to note that while direct georeferencing without GCPs can produce acceptable altimetric accuracy, (Bertin et al., 2022a) demonstrated the possibility of elevation biases. Their results emphasized the importance of considering the inclusion of at least one GCP, also considered in their previous research (Bertin et al., 2020), to control potential elevation biases and ensure greater accuracy. However, adding more GCPs during the photogrammetric block adjustment process gradually improved photogrammetric quality as more GCPs were added. It is noteworthy that all these experiments were conducted in homogeneous geographical environments, so the topographic factor did not significantly influence georeferencing error.

The accuracy of a UAV's position estimation with an RTK-GNSS receiver is the key determinant of UAV applicability for topographic operations. In the study by (Czyża et al., 2023), they demonstrated the ability of the RTK-GNSS receiver to provide precise positioning results concerning the planned flight trajectory, with a maximum discrepancy of 0.05m, indicating that the UAV was able to achieve precise and reliable results, with these measurements carried out in open terrain. However, it is important to consider that spatial data acquisition in areas with a more complex structure would lead to lower stability in the correction method used due to the UAV's inaccurate positioning during data acquisition. As a result, there is a risk of incomplete data acquisition for the entire area, as well as incorrect execution of assumed lateral and longitudinal coverage. Based on this reality, this study primarily focuses on the need to experiment with the optimal

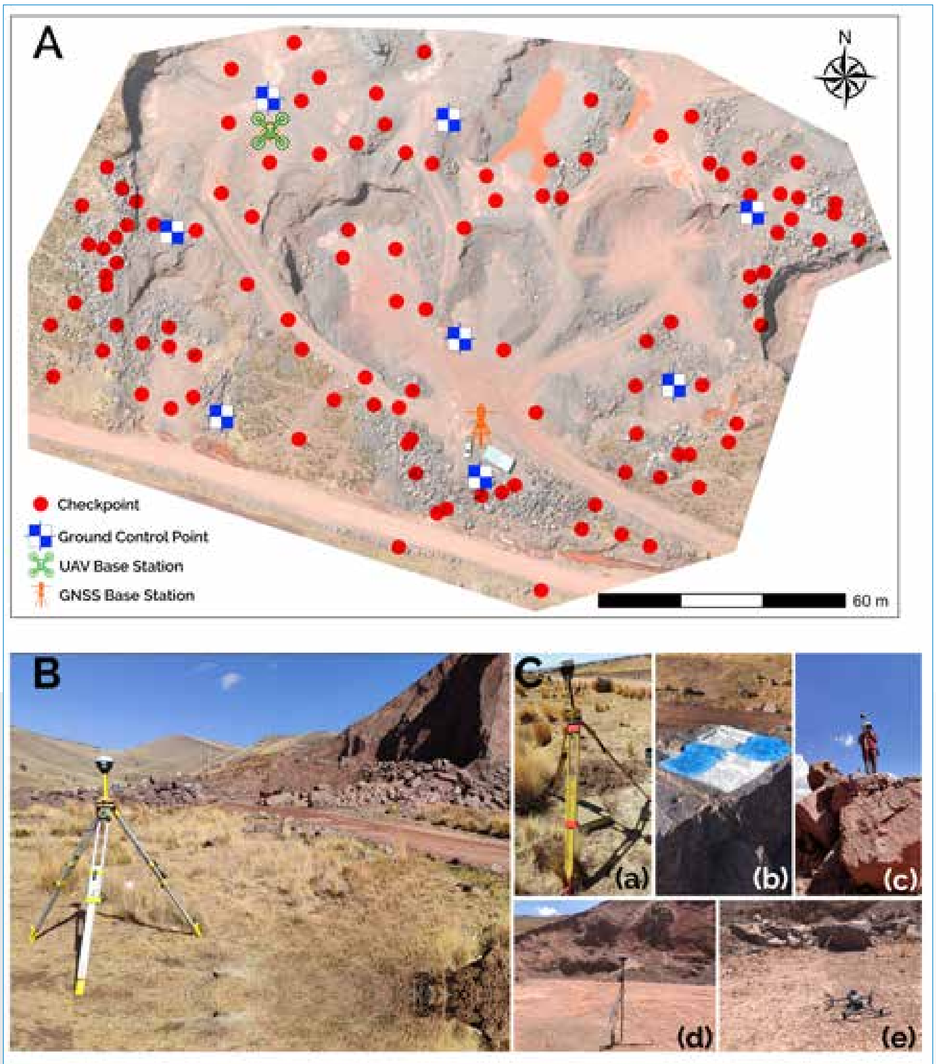

Fig. 2 - (A) Simplified map of the research area. (B) Photograph of the specific area under study. (C) Composed of five images from the research. Image (a) highlights the Class C geodetic point. Image (b) shows the photogrammetric target. The measurement of control points in the field is illustrated in image (c). The D-RTK2 base station is visible in image (d), while image (e) displays the DJI Mavic 3 Enterprise RTK drone.

number of GCPs with an RTK-enabled UAV to achieve a photogrammetric block error in the decimeter range, applied in a complex geographical environment.

Materials and Methods

Study Area

The study area presented in this research is located in southern Peru, specifically in the Puno region, considered a topographically complex zone due to its mountainous and rugged terrain. The study area is situated in the city of San Miguel. Specifically, the area in question corresponds to the Mucra rock quarry, approximately 14 hectares in extent, with an elevation difference of 80 meters and an average elevation of 3825 meters above sea level.

DIDA: Fig. 1 - Study Area. Projection coordinate system: WGS_1984_UTM_zone_19S.

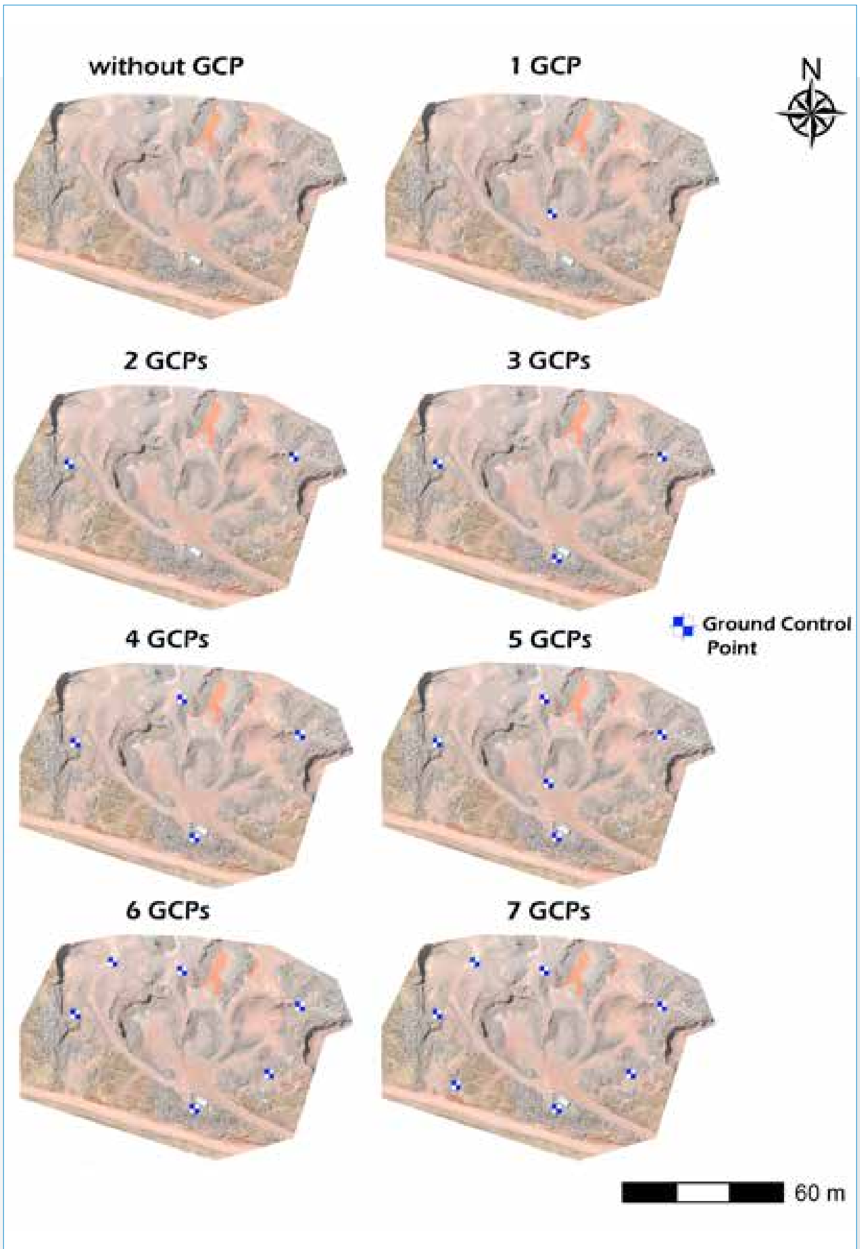

Fig. 3. Distribution scenarios of GCPs from 0 to 7 GCPs.

Data Acquisition

The field research was divided into two phases: terrestrial data collection on October 2, 2023, and aerial data collection on October 4, 2023. Both phases experienced sunny weather, with a constant wind speed of 3 m/s and gusts reaching up to 7 m/s, particularly during the second phase.

The first phase began with measurements of two geodetic points of Class C marked with concrete monuments, featuring a bronze plate of 70 mm diameter inscribed with the point codes PUN11339 and PUN11340. Their coordinates were captured using two GNSS receivers (Emblid RS2) capable of receiving GPS signals (QZSS L1C/A -L2C), GLONASS (L10F-L2OF), BeiDou (B1I-B2I), and Galileo (E1/BC -E5b). These receivers were set up as a base station with static relative horizontal positioning of ±3 mm+0.5ppm (parts per million), i.e., 1 mm per 1000 m, and vertical positioning of ±5 mm+1ppm over periods of 5:02:00 hours and 4:11:15 hours, respectively. From these, coordinates of 117 photogrammetric targets (0.50 x 0.50 m) were collected for use as GCPs and CPs. Each photogrammetric target was observed with a mobile GNSS receiver (Emblid RS2) with relative RTK kinematic positioning in horizontal ±8 mm+1ppm and vertical ±14 mm+1ppm for a duration of 30 seconds. It is noteworthy that the coordinates were recorded within the reference frame provided by the WGS84 system. To post-process the static observations, corrections were made using the reference base, the Permanent Tracking Station (ERP) of the National

Geographic Institute (IGN) with coding PU02.
Aerial imagery acquisition for photogrammetry was carried out using a Mavic 3 Enterprise RTK quadcopter by Da Jiang Innovations (DJI) with a maximum takeoff weight of 1050 grams. Utilizing the GNSS module, the DJI Mavic 3E RTK is capable of receiving GPS satellites (L1 C/A-L2-L5), BEIDOU (B1-B2-B3), GLONASS (F1-F2), Galileo (E1-E5A-E5B), providing real-time direct georeferencing of images with a horizontal positioning accuracy of ±0.10 m and vertical accuracy of ±0.10 m.
Flight planning was carried out using the UAV control, which features the DJI Pilot 2 application. We selected a flight plan that captures 3D images, enabling double-grid flights. The entire study area was covered by an autonomous double-grid flight at a constant altitude of 95m with a constant speed of 3 m/s and a lateral and frontal overlap ratio of 85%, with the stabilizer angle set at 30° from the vertical to eliminate elevation error (Štroner et al., 2021). This ensured an ortho GSD (Ground Sampling Distance) of 2.01 cm/pixel and an oblique GSD of 2.33 cm/pixel. The UAV is equipped with a camera featuring a 4/3-inch CMOS sensor and a resolution of 20 megapixels. It is notable for its balance of size and performance, capturing sharp details and vibrant colors, producing images with a resolution of 5280 x 3856 pixels.

Evaluation Scenarios for Control Points
To study the optimal configuration and quantity of

Category	Specifications
Moldel	DJI Mavic 3E RTK
Camera	20 mega pixeles
Hovering Accuracy (P-mode with GPS)	Vertical: ±0,1 m (with RTK)
	Horizontal: ±0,1 m (with RTK)
RTK Positioning Accuracy when RTK enabled and fixed	Vertical: 1.5 cm and 1ppm
	Horizontal: 1 cm and 1ppm
Signals Tracked:	GPS (L1 C/A-L2-L5), BEIDOU(B1-B2-B3), GLONASS(F1-F2), Galileo (E1-E5A- E5B)

Tab. 1 - UAV Specifications.

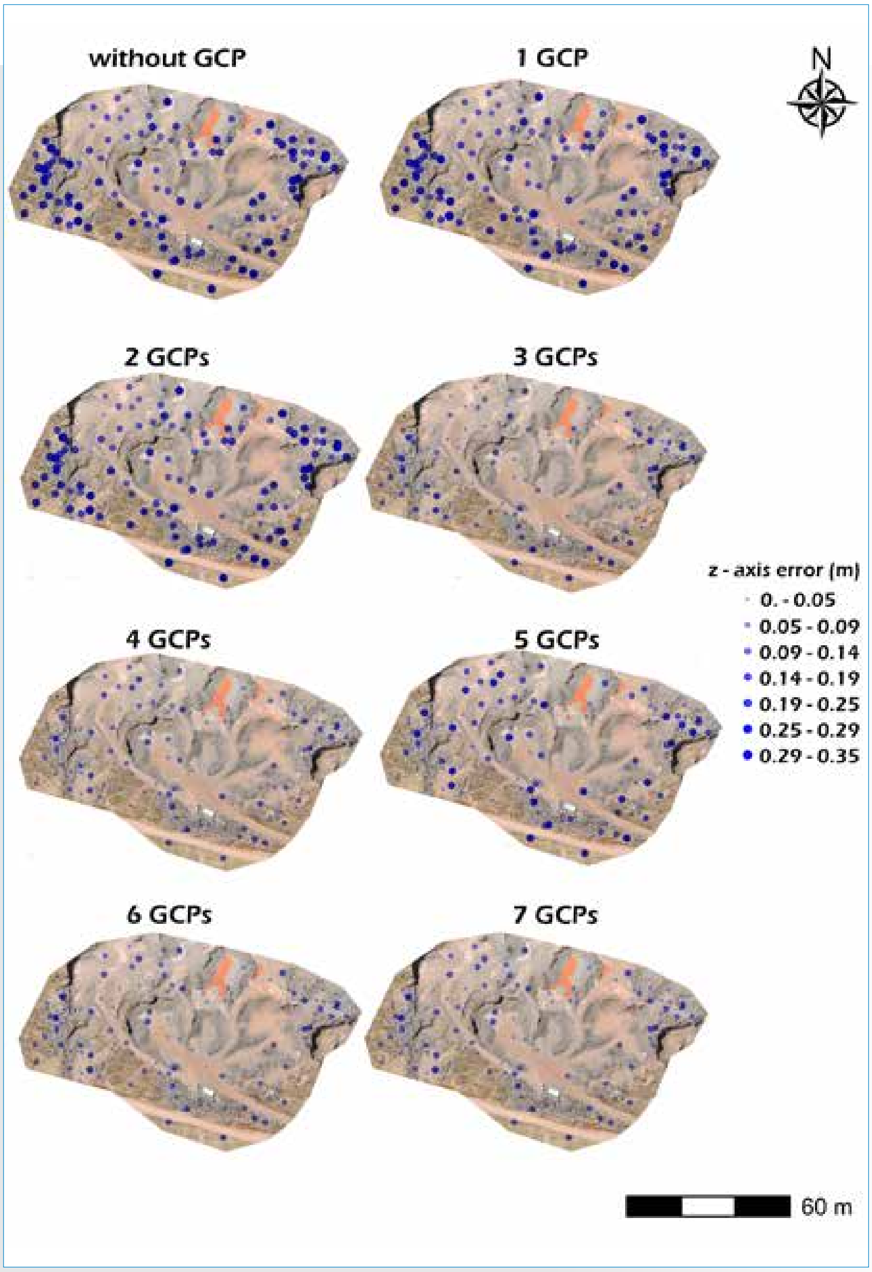

Fig. 4 - Spatial Configuration of Absolute Errors in the Z Axis for Each GCP Scenario.

GCPs, eight test scenarios were proposed. In each scenario, the number of GCPs was incremented by one, starting from 0 up to 7 GCPs throughout the study area. In the initial scenario, no GCPs were used. The use of oblique images and the implementation of double-grid flight plans ensure a high degree of accuracy without requiring the inclusion of GCPs (Taddia et al., 2020). In the second scenario, current literature recommendations were considered, suggesting that adding a single point located in the center can achieve global accuracy (RMSE) comparable to traditional photogrammetry, which relies on the presence of numerous well-distributed GCPs (Bertin et al., 2022a). The third scenario followed the suggestion from (Zhang et al., 2022a), which indicates that placing GCPs on two sides of an object may enhance calibration more than placing GCPs around it. Similarly, (Oniga et al., 2020) highlight the importance of placing GCPs in corners but warn against positioning them too far from the corners of the area of interest. Starting from the fourth scenario, which includes 3 GCPs, the design was based on the study by (Villanueva & Blanco, 2019) which emphasizes that as GCPs are distributed more widely across an area, errors will be reduced, whereas a more concentrated GCP placement increases terrain error.

$$N := \frac{k^2 \cdot s^2}{D^2} \quad \text{(a)}$$

N: number of required GCPs
k: confidence coefficient, generally 2 for a 95% confidence level
s: standard deviation of the distance between field-measured control points and known coordinates
D: desired vertical accuracy

Photogrammetric Information Processing

Pix4D software with an educational license was used for processing through the Structure from Motion (SfM) technique. One of the benefits provided by the Pix4D interface is that it is largely automated. The DJI Mavic 3 Enterprise RTK UAV uses the WGS84 coordinate system for both flight navigation and digital image geotagging. Therefore, in the initial stage, the coordinate system of the 991 uploaded images was not modified. In Pix4D, the SfM photogrammetry processing procedure consists of three stages. In the first stage, the software performed key point correlation. During this phase, characteristic points in the images were identified, which allows for establishing correspondences between images, creating an initial three-dimensional dataset. After key point identification, automatic aerial triangulation was carried out using the precise position information provided by the RTK receiver mounted on the UAV. To enhance three-dimensional accuracy, the software performed Block Adjustment. This combination resulted in a three-dimensional point cloud representing the point cloud captured by the UAV. At this stage, the software offers the option to generate the key point image scale: complete, fast, or custom. Initially, the second option was considered to expedite processing. This stage had a processing time of 4 hours. Once the procedure was completed, the coordinates of the CPs and GCPs were imported. Unlike the previously mentioned processing, the first option was chosen here. Unlike the fast processing, this option identifies and correlates GCPs in the images, establishing their position in the three-dimensional model based on their known coordinates, while in the block adjustment, the GCP information is taken into account, optimizing the position and orientation of the cameras to improve the alignment of the model with the actual coordinates of the ground control points. The second and third stages involved point cloud densification and generation of final products such as the Digital Surface Model (DSM) and orthophotos, utilizing the necessary information provided by the RTK-GNSS system. This procedure was carried out for all planned scenarios.

Component	Specification
CPU	AMD Ryzen 5 5600X 6-Core Processor
GPU	Radeon RX 570 Series
RAM	16 GB DDR4-2666 MHz
Storage	2TB
Average Processing Time	8 hours and 9 minutes

Tab. 2 - Processing Computer Specifications.

Quality Control of Measurements

To evaluate the results, error metrics were used, such as the Mean Error (ME), which is the arithmetic mean of the errors in each dimension; the Mean Standard Deviation (SDE), which measures the variability of the errors in each dimension; and the Root Mean Square Error (RMSE), which is a measure of the overall accuracy of the model, combining ME and SDE into a single statistical measure.

$$SDE := \sqrt{\frac{1}{n} \cdot \sum_{i=1}^{n} \left(y_i - x_i\right)^2}$$

(b)

$$ME := \frac{1}{n} \cdot \sum_{i=1}^{n} \left(y_i - x_i\right)$$

(c)

$$RMSE := \sqrt{\frac{1}{n} \cdot \sum_{i=1}^{n} \left(y_i - x_i\right)^2}$$

(d)

n: represents the number of CPs considered.
y_i: are the X, Y, and Z coordinates extracted from the photogrammetric block.
x_i: are the X, Y, and Z coordinates measured with differential GPS.

Results

Assessment of the Model Using Root Mean Square Error (RMSE)

The discrepancies within the set of 117 control points are detailed in Table 3, and the absolute differences in the Z-axis are visualized in *Figure* 4. When using only the UAV camera information without incorporating GCPs, the Mean Error (ME), calculated using equation (a), showed reduced values in the horizontal axes (ME x = 0.0693 m, ME y = 0.0686 m) compared to the vertical axis (ME z = -0.1781 m), which exhibited a high magnitude. Additionally, the Mean Standard Deviation (SDE), derived from equation (b), followed the same trend, with values of 0.0141 m, 0.0146 m, and 0.0664 m for the x, y, and z axes, respectively. The RMSE, calculated using equation (d), also maintained this sequence, with values of 0.0707 m, 0.0701 m, and 0.1900 m for the x, y, and z axes, respectively. In summary, these statistics highlight that the photogrammetric block captured using DG exhibits high bias and relatively high variability; the most notable discrepancies are observed in the Z-axis, which are characteristic of a surface study

		Average error (m)		
GCP number	Configuration	*x axis*	*y axis*	*z axis*
0	-	0.0693	0.0686	-0.1781
1	Center	0.0664	0.0615	-0.1692
2	Borders	0.0590	0.0583	-0.1651
3	Borders	-0.0161	-0.0079	-0.0426
4	Borders	-0.0139	-0.0060	0.0004
5	Borders + Center	-0.0090	-0.0018	0.0072
6	Borders	-0.0164	-0.0020	-0.0160
7	Borders	-0.0160	-0.0041	-0.0110

	Deviation standard (m)			Mean square error (m)		
GCP number	*x axis*	*y axis*	*z axis*	*x axis*	*y axis*	*z axis*
0	0.0141	0.0146	0.0664	0.0707	0.0701	0.1900
1	0.0144	0.0145	0.0662	0.0679	0.0632	0.1816
2	0.0142	0.0146	0.0655	0.0607	0.0601	0.1776
3	0.0140	0.0148	0.0663	0.0214	0.0168	0.0788
4	0.0140	0.0149	0.0666	0.0197	0.0160	0.0666
5	0.0139	0.0147	0.0668	0.0166	0.0149	0.0672
6	0.0137	0.0149	0.0667	0.0214	0.0151	0.0686
7	0.0137	0.0149	0.0669	0.0211	0.0155	0.0678

Tab. 3 - Error Analysis for the Seven Tested GCP Scenarios, Detailing the Configuration and Number of GCPs Used, as Well as the Resulting Error Metrics in the Three Dimensions.

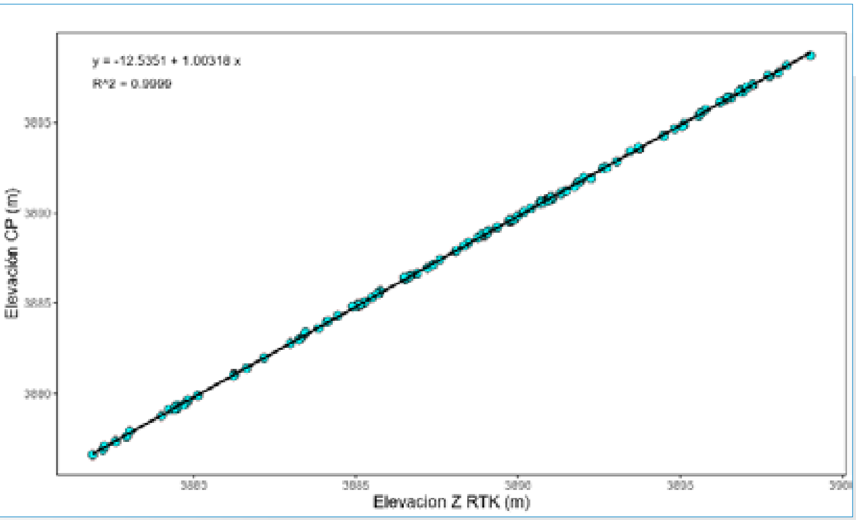

Fig. 5 - Linear Adjustment Function Between CP Elevations and DSM Elevations in the Absence of GCPs.

conducted with UAVs.
Precision assessment is carried out using error metrics presented in equations (b), (c), and (d), with results detailed in Table 3. Regarding the Mean Error (ME), the inclusion of two GCPs had minimal impact, with discrepancies of 0.0103 m, 0.0103 m, and -0.0129 m in the X, Y, and Z axes, respectively. However, with the addition of three GCPs, the ME decreased significantly, showing reductions of 0.0751 m, 0.0662 m, and -0.1226 m for the X, Y, and Z axes, compared to the two-GCP scenario. No substantial changes were observed beyond this number of control points.
Next, the residual error, characterized by the Standard Deviation (SDE), showed very similar values for all scenarios, as detailed in Table 3. The total error is described through the Root Mean Square Error (RMSE), which followed the same trend as the ME by significantly decreasing with the addition of three GCPs across all three axes. When comparing the resulting model with zero GCPs, differences of 0.0494 m for the X axis, 0.0533 m for the Y axis, and 0.1113 m for the Z axis were observed, with the latter experiencing a substantial reduction.
The implementation of onboard RTK, combined with a minimal number of GCPs, shows a positive impact on elevation accuracy, as illustrated in *Figure* 4. Throughout the 8 evaluated scenarios, it is evident that the most significant absolute errors are located in areas with abrupt elevation changes. In scenarios 1 and 5, where a single GCP is placed in the center, no noticeable reduction in RMSE is observed. On the other hand, in scenarios 3 and 4, where an edge configuration for the GCPs is used, a notable improvement in RMSE reduction is achieved.
Experimental results exploring the impact of GCP quantity on the three axes are presented in Table 3. In all GCP scenarios, it was observed that the error in the vertical dimension of the control point was greater than the error in the horizontal dimension. Both vertical and horizontal errors exhibited a decreasing trend as the number of GCPs increased. Specifically, a significant decrease in vertical error was noted with three GCPs.
Findings from the linear regression analysis highlight a strong and positive correlation between the elevation calculated using the onboard GNSS RTK navigation system of the UAV and the ground

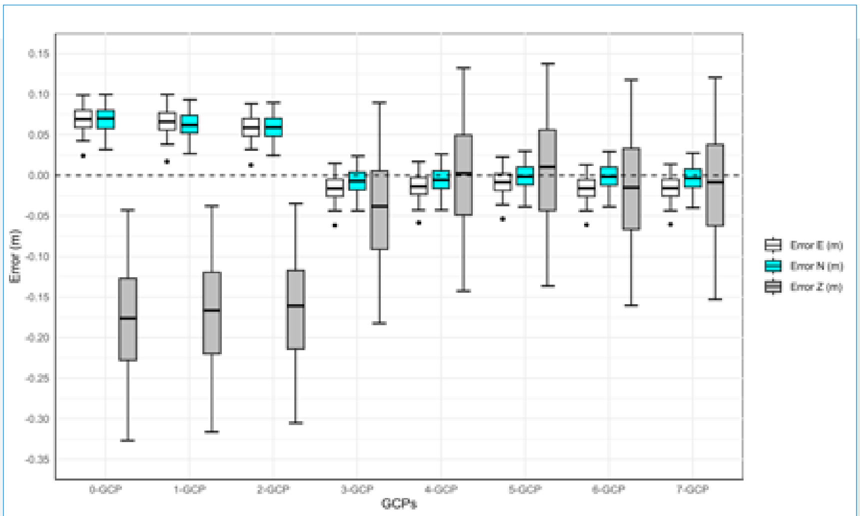

Fig. 6 - The difference between the CP and the 8 scenarios is illustrated using box plots. In these charts, the horizontal line denotes the median, the bottom of the box represents the 25th percentile, and the top reflects the 75th percentile. The "whiskers" extend up to 1.5 times the interquartile range (IQR) in both directions. Additionally, the black circles indicate outliers.

measurements obtained with GNSS RTK. The high coefficient of determination ($R^2 > 0.99$) underscores the robustness of this relationship, demonstrating the consistency and accuracy of the elevation measurements performed by both methodologies.

With the aim of proposing practical improvements for achieving more accurate UAV photogrammetry, this study not only addressed the number of ground control points (GCPs) but also examined the distance between the control points and the GCPs. For the evaluation, two Digital Surface Models (DSM) generated from three and four GCPs, previously identified as those with the minimum error, were considered. *Figure* 7 illustrates the relationship between the horizontal error of the control points and the distance to the nearest GCP. *Figure 7a* corresponds to 3 GCPs, while *Figure* 7b represents 4 GCPs. The resulting evaluation coefficient was less than 0.05, indicating that there is no relationship between the horizontal error and the distance between the GCPs and the control points.

Statistical Analysis

The focus of the statistical analysis was directed toward the vertical axis rather than the horizontal. This is because accurately quantifying elevation is more challenging than determining horizontal position using GNSS technologies. Errors are significantly smaller when satellites triangulate a horizontal point on the Earth's surface compared to doing so with a vertical point at a certain distance above the surface. In *figure* 6, histograms of the vertical differences between the control points and those captured by the UAV in RTK mode are shown for configurations of 0 and 4 GCPs, respectively. In *figure* 6a, the mean value of -0.0139 m suggests a systematically biased distribution. In contrast, *figure* 6b shows a mean value of -0.025 m, indicating that adding 4 GCPs helps to reduce vertical error. A normality test according to Shapiro-Wilk was performed for datasets with 116 and 112 observations corresponding to 0 and 4 GCPs, respectively. The results revealed test statistics (W) of 0.98893 and 0.999, indicating a strong approximation to a normal distribution, as both values are close to 1. Additionally, the associated p-values were 0.4627 and 0.5312, exceeding the significance threshold of 0.05. Therefore, there is insufficient evidence to reject the null hypothesis of normality in either case.

Fig. 8 - Histograms of Elevation Differences Between CP and UAV-RTK with 0 and 4 GCPs and Their Gaussian Fit.

A one-sample t-test was conducted, as shown in Table 4, with the premise that there is no significant difference between the mean and the test value of 0. Tests were

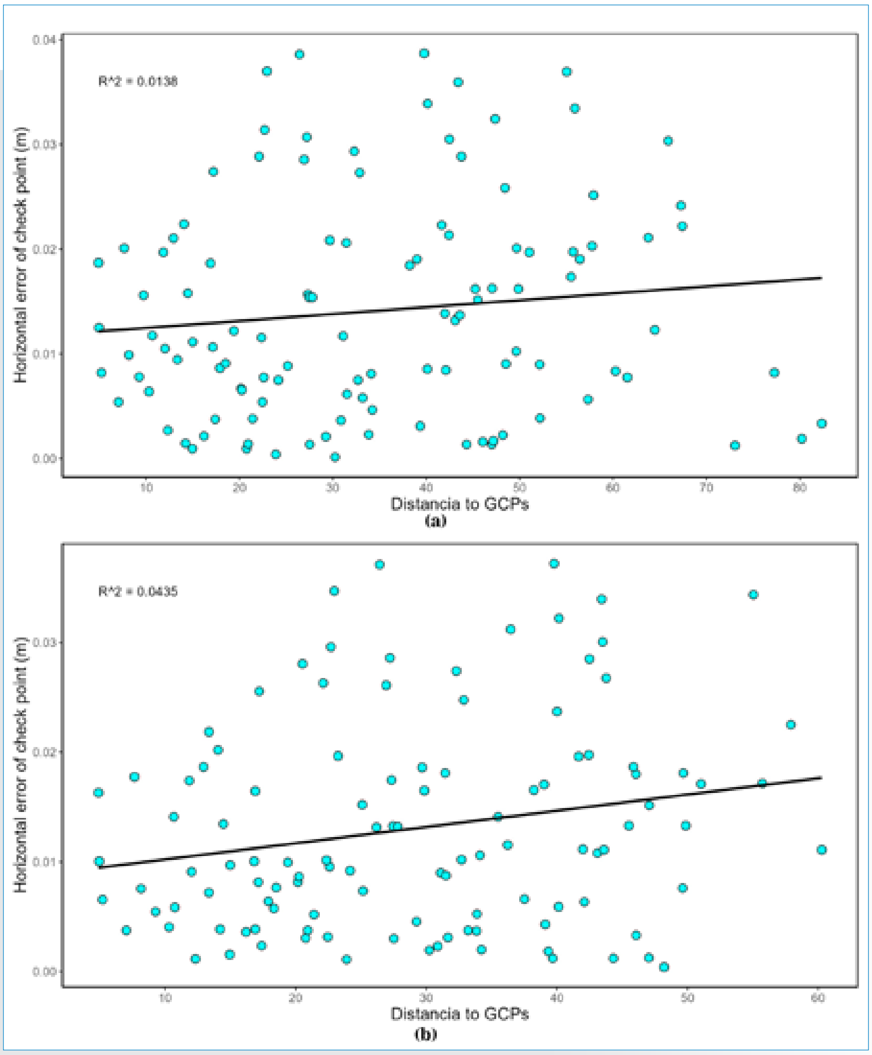

Fig. 7 - Relationship between the error and the distance between GCPs and CPs: (a) horizontal and (b) vertical.

performed for three different conditions with zero, two, and four GCPs, respectively.
The t-values were significantly different, with -29.064, -26.938, and 0.058 for zero, two, and four GCPs, respectively, suggesting that the number of GCPs statistically affects the means. The degrees of freedom decreased as the number of GCPs increased (116, 114, 112). The significance values were extremely low (0.005 and 0.005) for zero and two GCPs, indicating strong evidence to reject the null hypothesis of equal means. However, for four GCPs, the significance was 0.954, which did not reach the threshold to reject the null hypothesis, so it was accepted. The mean differences were consistently negative, and the 95% confidence intervals excluded 0 in all conditions, supporting the existence of significant differences. In summary, these results suggest that the number of GCPs plays a crucial role in the observed variations in the dataset.

Discussion

Remote sensing through UAVs is essential in various fields, but its effectiveness is compromised if accuracy is not ensured. Direct georeferencing can enhance the effectiveness of UAV measurements. In this regard, the results obtained are examined, and measures are proposed to improve the accuracy of various projects that present different demands regarding terrain resolution, as the required accuracy varies depending on the objective of generating the DSM. Consequently, relying solely on DG might not meet high precision standards.
After conducting tests across the 8 initially established scenarios, each model was evaluated using RMSE. The vertical and horizontal RMSE values obtained through DG, with an ortho resolution of 2.01 cm/pixel and an oblique resolution of 2.33 cm/pixel, were 0.07 m and 0.19 m, respectively. It is important to note that the accuracy of the results without GCPs was highly influenced by the accuracy of the image position data. Therefore, it can be said that the flight configurations designed based on current literature (Liu et al., 2022), such as the double grid flight combined with oblique and nadir images, along with a front and horizontal overlap of 85%, did not exponentially aid in error reduction. In cases of rugged topography, the use of GCPs is suggested as the best option.
Initially, the scenario without GCP was compared with one that included a single GCP in the center of the area, where no significant disparities were detected between the two. The study by (Bertin et al., 2022a) revealed that adding a single GCP in the center of the area helps reduce RMSE in the Z direction, while (Cho & Lee, 2023) indicate that, regardless of its location, a GCP can effectively eliminate vertical bias during processing. Both studies agree that including a GCP reduces RMSE.
However, these findings differ from the results of previous research by (Stott et al., 2020b), which concluded that a single GCP does not improve summarized error statistics, consistent with this study's results of not finding a significant difference in RMSE between the no-GCP scenario and the 1-GCP scenario. This discrepancy may be due to the topographical complexity of the study area.
Figure 4 shows the absolute errors in the Z direction, characterized by significant variations in elevation, indicating that the largest errors are concentrated in areas with greater topographic roughness. This suggests that the latter affects the quality of the photogrammetric block.
This is consistent with findings from other authors (Stott et al., 2020a) and (Czyża et al., 2023), who report that in areas with relatively steep slopes, there is an inherent potential for elevation errors due to incorrect drone positioning during spatial data acquisition. (Kim et al., 2023), studied RTK-GNSS positioning of a UAV in an open-pit copper mine, finding that RTK-GNSS positioning is accurate in terms of both the relative camera location error and the image mapping error based on GCPs, with an average total error of 1.6 cm, which is mainly attributable to external factors, including weather conditions. The influence of these factors can be minimized but not completely eliminated in field studies. Based on the results of the aforementioned authors, we can rule out that the errors in the photogrammetric block predominantly stem from UAV positioning.(Stott et al., 2020b), noted that in digital photogrammetry, topographic geomorphological datasets derived from SfM may exhibit complex spatially distributed errors due to software interpretation, which can be reduced by GCPs providing additional external information about the geometry of the reconstructed scene. During

the optimization process, the software improves camera positioning accuracy and reduces nonlinear distortions in the project by incorporating GCPs. Additionally, part of the photogrammetric block error may have been due to the use of natural features as GCPs and CPs considered in this project. (Yang et al., 2022), observed that using natural feature points as control points resulted in high error in the Z direction of the control points. This instability is determined by the quality of the natural point, as its real position is not easily identifiable in aerial images and often exhibits some deviation. The location of characteristic points in the image depends on the subjective judgment of professionals, which can introduce significant error margins due to human factors. Therefore, the use of natural features for aerial photogrammetry is not recommended when high precision is required.

In the study by (Czyża et al., 2023), the importance of using GCPs with DG systems is highlighted, especially in areas with complex characteristics such as variations in vegetation cover, steep topography, and texture changes. On the other hand, (Liu et al., 2022), suggests using two to three GCPs to achieve an optimal balance between accuracy and efficiency. When comparing the photogrammetric block with two GCPs to one GCP, similar results were obtained, which did not differ significantly from the case with zero GCPs. Consequently, we can affirm that in complex topographies with varying heights, considerable precision is not achieved, which differs from the studies of (Liu et al., 2022). In this study, the best results were obtained with three GCPs. This finding suggests that using at least three GCPs results in a significant improvement in the calibration of the photogrammetric block, with further benefits from including a greater number of evenly distributed GCPs.

The analysis of the results presented in Table 3 allows us to conclude that the optimal number of GCPs is between 4 and 5, which provided the best results. However, it is necessary to consider that an excessive number of GCPs is unnecessary, as they do not improve the summarized error statistics, since the error tends to increase, which is also explained by (Zhang et al., 2022b).

The shape of the GCP configuration was a main factor affecting the precision of GCP calibration. Previous studies suggested placing GCPs at the edges as optimal. However, experiments where a GCP was placed in the center did not reflect the improvements explained by (Bertin et al., 2022b) which is also supported by (Park & Yeom, 2022), Consequently, we can assert that in this particular study, placing a GCP in the center did not

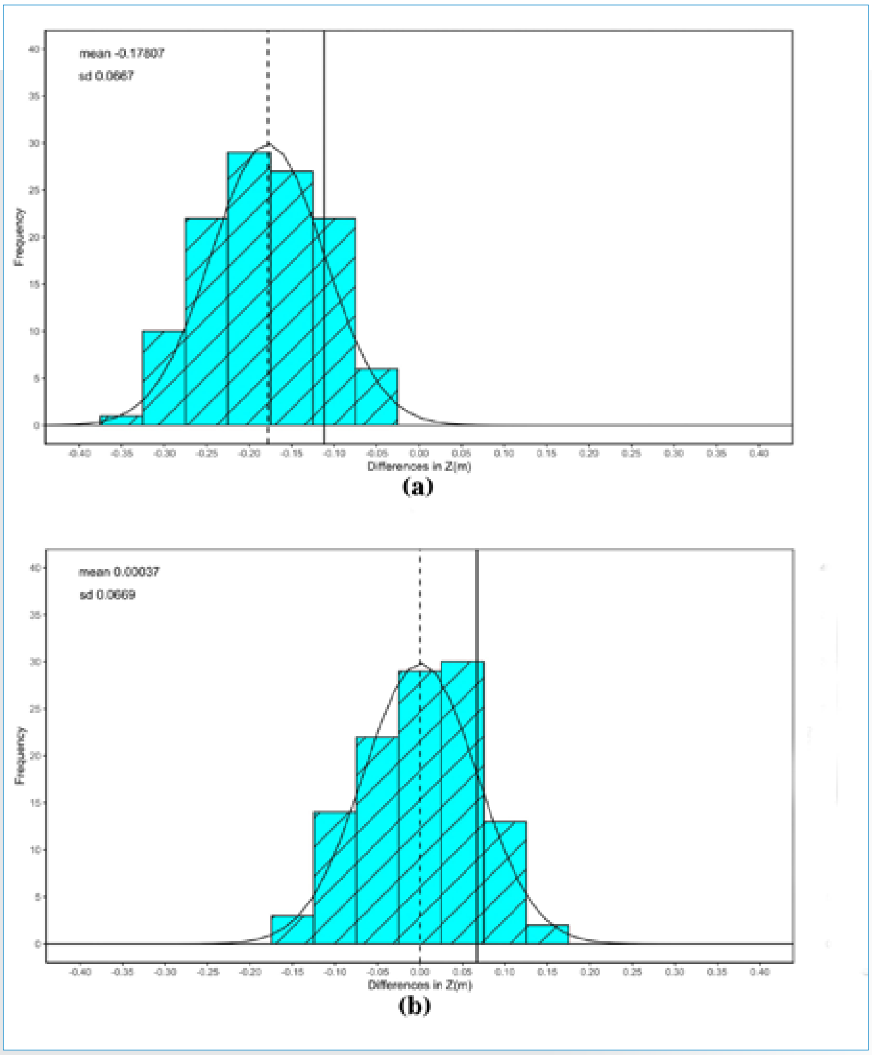

Fig. 8 - Histograms of Elevation Differences Between CP and UAV-RTK with 0 and 4 GCPs and Their Gaussian Fit.

provide improvements, similar to the findings of (Cho & Lee, 2023). *Figures 7a* and *7b* show the linear adjustment to determine if the horizontal and vertical errors of the control points decrease as the distance from the nearest GCP increases. In the study carried out by (Zhang et al., 2022b), reported that the horizontal error tended to increase as the distance between the GCP and CP increased. In our study, with the inclusion of 1 GCP in the center, this distance decreases, which would result in a smaller relationship between the horizontal error of the control points and the distance to the nearest GCP. Conversely, *Figures 7a* and *7b* do not show this relationship, similar to (Liu et al., 2022). The methodology used in UAV photogrammetry that requires high precision is still limited in the field of engineering. This is due to the uncertain survey procedure caused by differences between various study sites. It is recommended that future studies consider a larger number of CPs, which is crucial for RMSE analysis and spatial verification of the area where the most errors occur. Another recommendation is to perform scheduled flights according to the surface, as it is challenging to consider flights at altitudes below 100 meters in areas with complex topography. This is an important factor, as (Pourreza et al., 2022b) reported that the accuracy of data collected by the UAV-RTK system depends on the flight altitude.

REFERENCES

Benassi, F., Dall'Asta, E., Diotri, F., Forlani, G., Cella, U. M. di, Roncella, R., & Santise, M. (2017). Testing accuracy and repeatability of UAV blocks oriented with gnss-supported aerial triangulation. *Remote Sensing*, *9*(2), 1–23. https://doi.org/10.3390/rs9020172

Bertin, S., Levy, B., Gee, T., & Delmas, P. (2020). Geomorphic change detection using cost-effective structure-from-motion photogrammetry: Evaluation of direct georeferencing from consumer-grade uas at orewa beach (new zealand). *Photogrammetric Engineering and Remote Sensing*, *86*(5), 289–298. https://doi.org/10.14358/PERS.86.5.289

Bertin, S., Stéphan, P., & Ammann, J. (2022a). Assessment of RTK Quadcopter and Structure-from-Motion Photogrammetry for Fine-Scale Monitoring of Coastal Topographic Complexity. *Remote Sensing*, *14*(7). https://doi.org/10.3390/rs14071679

Bertin, S., Stéphan, P., & Ammann, J. (2022b). Evaluación de cuadricóptero RTK y fotogrametría de estructura a partir del movimiento para el monitoreo a escala fina de la complejidad topográfica costera. *Remote Sensing*, *14*(7). https://doi.org/10.3390/rs14071679

Cho, J. M., & Lee, B. K. (2023). GCP and PPK Utilization Plan to Deal with RTK Signal Interruption in RTK-UAV Photogrammetry. *Drones*, *7*(4). https://doi.org/10.3390/drones7040265

Czyża, S., Szuniewicz, K., Kowalczyk, K., Dumalski, A., Ogrodniczak, M., & Zieleniewicz, Ł. (2023). Assessment of Accuracy in Unmanned Aerial Vehicle (UAV) Pose Estimation with the REAL-Time Kinematic (RTK) Method on the Example of DJI Matrice 300 RTK. *Sensors*, *23*(4). https://doi.org/10.3390/s23042092

Elkhrachy, I. (2021). Accuracy Assessment of Low-Cost Unmanned Aerial Vehicle (UAV) Photogrammetry. *Alexandria Engineering Journal*, *60*(6), 5579–5590. https://doi.org/10.1016/j.aej.2021.04.011

Kim, H., Hyun, C. U., Park, H. D., & Cha, J. (2023). Image Mapping Accuracy Evaluation Using UAV with Standalone, Differential (RTK), and PPP GNSS Positioning Techniques in an Abandoned Mine Site. *Sensors*, *23*(13). https://doi.org/10.3390/s23135858

Liu, X., Lian, X., Yang, W., Wang, F., Han, Y., & Zhang, Y. (2022). Accuracy Assessment of a UAV Direct Georeferencing Method and Impact of the Configuration of Ground Control Points. *Drones*, *6*(2). https://doi.org/10.3390/drones6020030

Oniga, V. E., Breaban, A. I., Pfeifer, N., & Chirila, C. (2020). Determining the suitable number of ground control points for UAS images georeferencing by varying number and spatial distribution. *Remote Sensing*, *12*(5). https://doi.org/10.3390/rs12050876

Padró, J. C., Carabassa, V., Balagué, J., Brotons, L., Alcañiz, J. M., & Pons, X. (2019). Monitoring opencast mine restorations using Unmanned Aerial System (UAS) imagery. *Science of the Total Environment*, *657*, 1602–1614. https://doi.org/10.1016/j.scitotenv.2018.12.156

Park, J. W., & Yeom, D. J. (2022). Method for establishing ground control points to realize UAV-based precision digital maps of earthwork sites. *Journal of Asian Architecture and Building Engineering*, *21*(1), 110–119. https://doi.org/10.1080/13467581.2020.1869023

Pourreza, M., Moradi, F., Khosravi, M., Deljouei, A., & Vanderhoof, M. K. (2022). GCPs-Free Photogrammetry for Estimating Tree Height and Crown Diameter in Arizona Cypress Plantation Using UAV-Mounted GNSS RTK. *Forests*, *13*(11). https://doi.org/10.3390/f13111905

Stott, E., Williams, R. D., & Hoey, T. B. (2020a). *Distribución de puntos de control terrestre para mapeo topográfico preciso a escala de kilómetros utilizando un vehículo aéreo no tripulado RTK-GNSS y fotogrametría SfM.* www.mdpi.com/journal/dronesTraducidodelinglésalespañol-www.onlinedoctranslator.com

Stott, E., Williams, R. D., & Hoey, T. B. (2020b). Ground control point distribution for accurate kilometre-scale topographic mapping using an rtk-gnss unmanned aerial vehicle and sfm photogrammetry. *Drones*, *4*(3), 1–21. https://doi.org/10.3390/drones4030055

Štroner, M., Urban, R., Seidl, J., Reindl, T., & Brouček, J. (2021). Photogrammetry using UAV-mounted GNSS RTK: Georeferencing strategies without GCPs. *Remote Sensing*, *13*(7). https://doi.org/10.3390/rs13071336

Taddia, Y., Stecchi, F., & Pellegrinelli, A. (2020). Coastal mapping using dji phantom 4 RTK in post-processing kinematic mode. *Drones*, *4*(2), 1–19. https://doi.org/10.3390/drones4020009

Villanueva, J. K. S., & Blanco, A. C. (2019). Optimization of ground control point (GCP) configuration for unmanned aerial vehicle (UAV) survey using structure from motion (SFM). *International Archives of the Photogrammetry, Remote Sensing and Spatial Information Sciences - ISPRS Archives*, *42*(4/W12), 167–174. https://doi.org/10.5194/isprs-archives-XLII-4-W12-167-2019

Yang, J., Li, X., Luo, L., Zhao, L., Wei, J., & Ma, T. (2022). New Supplementary Photography Methods after the Anomalous of Ground Control Points in UAV Structure-from-Motion

Conclusions

This study investigated the impact of Ground Control Points (GCPs) on the measurement quality of a photogrammetric block in highly rugged terrain, using a UAV equipped with RTK positioning capabilities.
The evaluation of a UAV in RTK mode without any GCPs resulted in horizontal and vertical RMSE values of 0.0704 meters and 0.1900 meters, respectively. These results indicate that an RTK-GNSS UAV alone is insufficient to achieve decimeter-level accuracy in photogrammetric blocks without GCPs.
Results from the seven test scenarios suggest that incorporating 3 to 5 GCPs distributed uniformly has a significant effect on the adjustment of the photogrammetric block, in contrast to scenarios with 1 or 2 GCPs, which do not show a significant difference compared to having no GCPs.
Prior knowledge regarding the optimal number and placement of GCPs is crucial to minimizing errors. It is recommended that future studies increase the number of control points to improve RMSE analysis and spatial error verification, and to plan flights based on the terrain surface. The results and recommendations presented are expected to benefit researchers and practitioners using UAV photogrammetry by providing more accurate and reliable data for their research and practical applications.

Photogrammetry. *Drones*, *6*(5). https://doi.org/10.3390/drones6050105
Zhang, K., Okazawa, H., Hayashi, K., Hayashi, T., Fiwa, L., & Maskey, S. (2022a). Optimization of Ground Control Point Distribution for Unmanned Aerial Vehicle Photogrammetry for Inaccessible Fields. *Sustainability (Switzerland)*, *14*(15). https://doi.org/10.3390/su14159505
Zhang, K., Okazawa, H., Hayashi, K., Hayashi, T., Fiwa, L., & Maskey, S. (2022b). Optimization of Ground Control Point Distribution for Unmanned Aerial Vehicle Photogrammetry for Inaccessible Fields. *Sustainability (Switzerland)*, *14*(15). https://doi.org/10.3390/su14159505

KEYWORDS
Direct Georeferencing; GCPs; Photogrammetric Block; Accuracy Evaluation

ABSTRACT
This study investigates the impact of using Ground Control Points (GCPs) on the measurement quality of photogrammetric blocks in high topographic roughness areas, captured with an RTK-enabled UAV. The research evaluates eight scenarios with varying numbers of GCPs to determine their effect on horizontal and vertical Root Mean Square Error (RMSE), Mean Error (ME), and Standard Deviation Error (SDE). The study area was characterized by high topographic roughness, with a UAV equipped with RTK GNSS used to capture images, and 117 control points (CP) established for accuracy assessment. The UAV was flown in a double grid pattern with nadir and oblique images, ensuring 85% overlap. The GCPs were distributed in different configurations across the area, ranging from zero to six GCPs per scenario. When no GCPs were used, the horizontal ME was 0.0693 m (X-axis) and 0.0686 m (Y-axis), while the vertical ME was significantly higher at -0.1781 m. The SDE followed a similar trend, with the vertical SDE being the highest. The RMSE values were 0.0707 m (X-axis), 0.0701 m (Y-axis), and 0.1900 m (Z-axis), indicating substantial bias and variability, particularly in the vertical axis. The inclusion of two GCPs had minimal impact on ME, but starting from three GCPs, ME decreased significantly, especially in the Z-axis. The SDE remained consistent across different GCP scenarios, and the RMSE showed a marked reduction with the addition of three GCPs, with no significant improvement observed beyond this number. The optimal number of GCPs was identified as four to five, providing the best accuracy results without an unnecessary increase in GCPs. The study confirmed that using RTK GNSS onboard UAVs enhances elevation accuracy, especially when coupled with a minimum number of GCPs. Significant errors were noted in areas with abrupt elevation changes, and the central placement of a single GCP did not significantly reduce RMSE. Linear regression analysis demonstrated a strong positive correlation between UAV RTK-derived elevations and terrestrial GNSS RTK measurements, with a high coefficient of determination ($R^2 > 0.99$). The spatial configuration of GCPs was crucial, with edge placements proving more effective than central ones. Histograms of vertical differences between control points and UAV RTK measurements indicated a systematic bias reduced with the addition of GCPs. The research also examined the relationship between control point error and distance to the nearest GCP, finding no significant correlation. This study underscores the importance of GCPs in improving the measurement quality of photogrammetric blocks in areas with high topographic roughness. Without GCPs, UAV RTK systems were insufficient for achieving decimeter-level accuracy. Including three to five GCPs significantly enhanced accuracy, with no substantial benefits beyond five GCPs. This finding suggests that an optimal GCP configuration balances the number and placement to minimize errors efficiently. The research provides practical recommendations for UAV photogrammetry, emphasizing the need for adequate GCPs in complex terrains. Future studies should consider increasing the number of control points for better RMSE analysis and spatial error verification, and flight planning based on surface characteristics is advised to improve data accuracy in topographically complex areas. The findings and recommendations presented in this study offer valuable insights for researchers and practitioners using UAV photogrammetry, contributing to more precise and reliable data for various applications.

AUTHOR
Kevin De Flué Pilco Lopez
kevin.pilco@upeu.edu.pe
Moisés Araca Chile

Peruvian Union University (UpeU)
Professional School of Civil Engineering
Heroes of the Pacific War Highway Km. 6.1 Chullunquiani, San Roman, Puno Peru